JOURNAL OF OPTOELECTRONICS AND ADVANCED MATERIALS Vol. 12, No. 3, March 2010, p. 528 - 534

Synthesis of copper nanopowders by transferred arc and non-transferred arc plasma systems

MU-GAP SHIN, DONG-WHA PARK*
Department of Chemical Engineering and Regional Innovation Center for Environmental Technology of Thermal Plasma (RIC-ETTP) INHA University, 253 Yonghyun-dong, Nam-gu, Incheon, 402-751, Korea.

Copper nanopowders were prepared from bulk material using a transferred arc plasma system. N_2 diluting gas flow rate was introduced as an experimental parameter. It was observed that as the flow rate of the diluting gas was increased, the oxidation level of the copper nanopowders was greatly reduced and the particle size was also decreased. Also, copper nanopowders were prepared using a non-transferred arc plasma system. The morphology and the particle size were changed by the flow rate of the N_2 added plasma gas, as it was confirmed by the results of the scanning electron microscopy (SEM), particle size analyzer (PSA), X-ray diffractometer (XRD), transmission electron microscopy (TEM), elemental analyzer (EA), and thermogravimetric analyzer (TGA). The experimental results of the two types of the plasma systems showed the remarkable differences. The evaporation rate of the bulk copper by the transferred arc plasma system was much higher than that of the non-transferred arc plasma system. The mean particle size of the particles prepared by the transferred arc was 98 nm while that of the particles prepared by the non-transferred arc was about 202 nm confirmed by PSA.

(Received June 21, 2009; accepted December 9, 2009)

Keywords: Transferred arc plasma, Non-transferred arc plasma, Copper, Nanopowders

1. Introduction

Pure copper nanopowder can be used as an inner electrode material of a Multi-Layer Ceramic Capacitor (MLCC) because of its excellent properties such as electrical, thermal conductivity and good electron spin resonance (ESR) [1]. Also the copper nanopowders were used as nanoprobes in medicine and bioanalytical fields [2]. The nanopowders were prepared by mechanical milling and chemical-mechanical milling [3], hydrothermal synthesis [4], chemical precipitation [5], spray pyrolysis [6]. The major method used in preparing nanopowders is the liquid phase method. However, this method has some limitations such as restraining the phase composition and very complex filtration and drying process [7]. Moreover, little progress has been made on synthesizing nano-sized powders because of difficulty in restraining oxidation and controlling the composition of the nano materials [8].

Recently, an innovative plasma processing technique has been developed for the preparation of the nanopowders by vapor phase reaction [9-14]. Thermal plasma methods have exceptional merits such as (a) high temperatures and energy densities, (b) rapid evaporation and quenching system, (c) clean and continuous process and (d) a wide range of starting materials [15, 16]. The plasma is rapidly cooled in the tail flame region. The supersaturation of vapor species which provides the driving force for particle condensation can be very high in the plasma tail, leading to the production of ultra fine particles through homogeneous nucleation [17]. The synthesis of metal nanopowders having a wide range of melting points is possible using a thermal plasma system [18].

The present paper reports that the copper nanopowders from bulk copper were prepared by thermal plasma systems. Additionally, the introduction of a diluting gas in the transferred arc plasma system was effective in controlling the particle sizes and decreasing oxidation. The morphologies and the particle sizes were analyzed depending on the plasma added gas and the collection position in case of the non-transferred arc plasma system.

2. Experimental

2.1 SYSTEM 1 (Transferred arc plasma system)

Fig. 1 shows a schematic diagram of the transferred arc plasma system. It consists of a DC generator, a quenching tube, a chamber, a tungsten crucible, a filter, a vacuum system and a plasma torch. The plasma torch consists of a water-cooled tungsten cathode and a copper anode. It can be moved up and down, forward and backward to control the distance between the plasma torch and the tungsten crucible. Bulk copper was used as raw material. Argon (Ar) gas was employed as the plasma gas. Nitrogen (N_2) gas was introduced as the diluting gas and

also used as the quenching gas. Raw material was easily evaporated by the high temperature in the plasma region, followed by rapid condensation in the quenching tube. In this experiment, the flow rate of the diluting gas was a critical parameter to control the particle sizes and the phase composition of the copper nanopowders. Before a run, the reactor was purged with N_2 for 10 minutes. The detailed experimental conditions are summarized in Table 1.

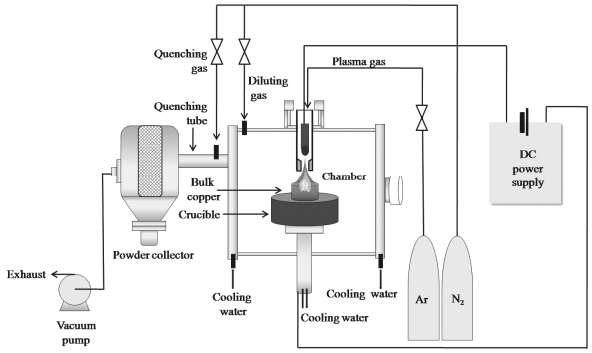

Fig. 1. Schematic diagram of transferred arc for the synthesis of Cu nanopowders.

Table 1. Experimental conditions for the synthesis of Cu nanopowders by transferred arc.

Experimental No.	1	2	3	4	5	6
Flow rate of plasma gas (Ar, l/min)	10	10	10	10	10	10
Flow rate of diluting gas (N_2, l/min)	0	50	100	150	200	250
Flow rate of quenching gas (N_2, l/min)	50	50	50	50	50	50
Operating current (A)	300	300	300	300	300	300
Voltage (V)	45	45	45	45	45	45

2.2 SYSTEM 2 (Non-transferred arc plasma system)

Fig. 2 shows an experimental setup, which consists of the DC generator, the chamber, the crucible, the vacuum system, and the plasma torch consisting of the water-cooled tungsten cathode and the copper anode. Bulk copper was also used as raw material the same as in the transferred arc plasma system. Argon (Ar) gas was employed as the major plasma gas. But it is difficult to evaporate bulk copper using only Ar plasma gas because of a high boiling point of copper. For this reason, nitrogen (N_2) gas was introduced as the added gas because N_2 molecule is easily dissociated to atomic nitrogen and it partially generates the required heat for the evaporation of bulk copper through the recombination of the atomic nitrogen. Thus, the flow rate of the N_2 added gas was a critical parameter to control the evaporation rate and the particle sizes. Also, we confirmed that the particle sizes and the phase composition of the copper nanopowders were different according to the collecting distance. Before the run, the system was purged with Ar for 10 minutes. The experimental conditions and the operating variables are indicated in Table 2.

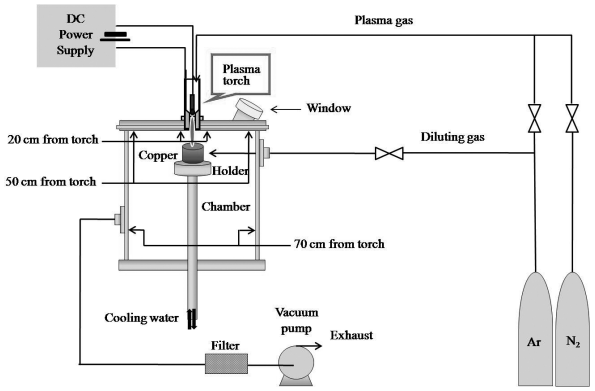

Fig. 2. Schematic diagram of non-transferred arc for the synthesis of Cu nanopowders.

Table 2. Experimental conditions for the synthesis of Cu nanopowders by non-transferred arc.

Experimental No.	7	8	9	10	11
Flow rate of plasma gas (Ar, l/min)	15	15	15	15	15
Flow rate of added gas (N_2, l/min)	1.0	1.5	2.0	1.0	1.0
Flow rate of diluting gas (Ar, l/min)	5	5	5	5	5
Collection position (cm from torch)	20	20	20	50	70
Operating current (A)	300	300	300	300	300
Voltage (V)	24	27	30	24	24

In this work, the prepared powder was obtained from the quenching tube in the case of system 1 and from the chamber wall in of system 2. Phase composition of the powder was analyzed by an X-ray Diffractometer (XRD, /MAX 2200V/PC/Rigaku), Energy Dispersive X-ray Spectrometer (EDX, S-4300/Hitachi Co.) and Transmission Electron Microscopy (TEM, JEM-2100F/Jeol Co.). The morphology and the particle size of the synthesized powder were observed by Scanning Electron Microscopy (SEM, S-4300/Hitachi Co.), a Light Scattering Particle Size Analyzer (PSA, ELS-Z2/Otsuka Co.), and an Elemental Analyzer (EA, 2400 Series CHNS/Perkin Elmer Co.). The thermal properties of the copper nanopowders were investigated using a Thermogravimetric Analyzer (TGA-SDTA, 851/ Mettler Toledo Co.).

3. Results and discussion

Generally, the copper nanopowders are red or brownish, according to their specific plasma absorption, but they readily change to black. This phenomenon can be explained by the oxidation of the surface of the copper powders. The formation and the growth of the copper oxide onto metallic copper powders can easily be sustained by the contact with oxygen. Hence, the synthesis of pure copper nanopowders is very difficult, and we had

to analyze the synthesized copper nanopowders as soon as possible before major oxidation occurred.

3.1 SYSTEM 1 (Transferred arc plasma system)

Fig. 3 shows SEM images of the selected copper nanopowders synthesized at the same operating conditions as in Table 1. All the powders showed spherical shapes because of surface energy. This indicates that these products were formed by melting, evaporation and the subsequent condensation of starting material. When the diluting gas was not introduced to the reactor, the prepared powder sizes were above 300 nm. However, as the flow rate of the diluting gas was increased, the size of the prepared powder was decreased. Especially, when the flow rate of the diluting gas was introduced at more than 200 l/min, most of the prepared powders were below 100 nm, super-nanopowders. When the flow rate of the introduced diluting gas was increased, the evaporation rate of bulk copper was decreased because the temperature of the molten copper was decreased. In other words, the diluting gas controls the concentration of the copper vapors and it decreases the collision rate among the copper vapors. It might be concluded that this phenomenon operated as a factor to control nucleation, so it led to a decrease in the size of the powders.

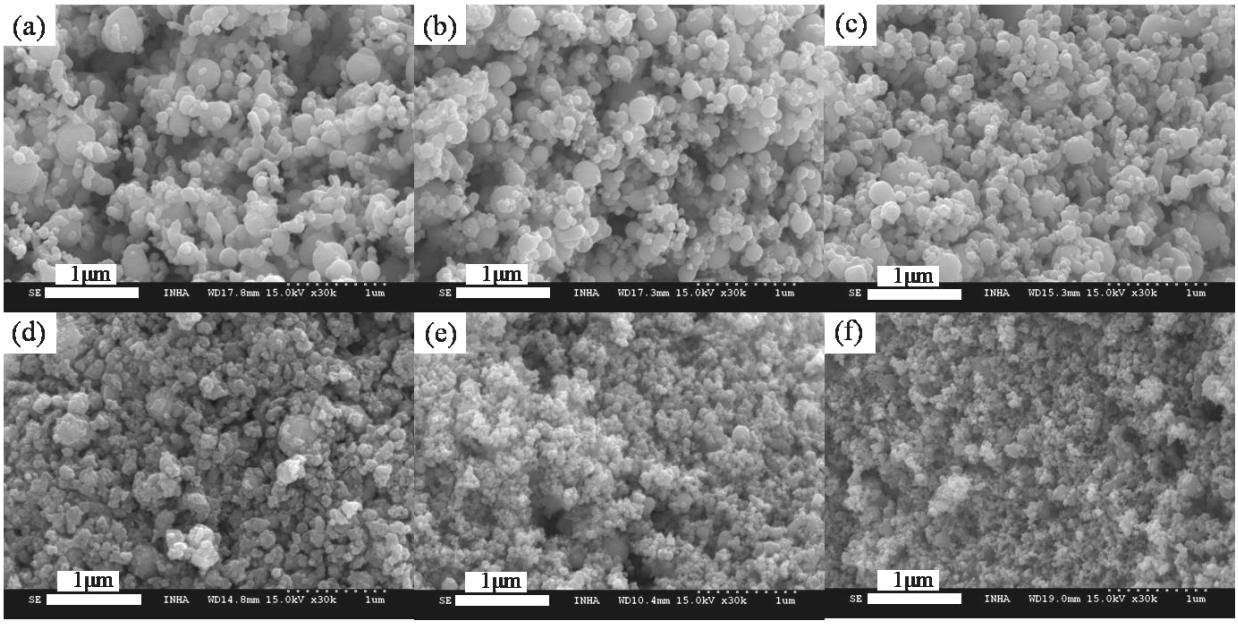

Fig. 3. SEM images of the powders, depending on the diluting gas by transferred arc : (a) No. 1 (b) No. 2 (c) No. 3 (d) No. 4 (e) No. 5 (f) No. 6

Fig. 4(a) shows PSA results of the synthesized powders at the same operating conditions as in Table 1. Even though the PSA results were kept with agglomeration in mind, the powder sizes were nano-scale powders. As the flow rate of the diluting gas was increased, the size of the prepared powder was decreased, as the results from Fig. 3 shown as well.

Fig. 4(b) shows an accumulative probability of the synthesized copper powders from the PSA results of experimental No. 6. This graph illustrates that all the sizes of the prepared powders were below 200 nm, and more than 80 % of the amount prepared from the copper powder was beneath 100 nm. From this result, the process of making super-nanopowders from bulk material is possible when using the transferred arc plasma system**.**

The phase composition of the synthesized powders is shown in Fig. 5 at the same operating conditions as in Table 1. When the diluting gas was not introduced, the peaks of the prepared powder were a mixture of a great quantity of the copper and a small amount of the copper oxide (Cu_2O). It might be explained that there were small leak points in this system. However, as the flow rate of the diluting gas was increased, the peaks of copper oxide were decreased and perfectly disappeared when the flow rate of the diluting gas was introduced above 200 l/min. From this result, it could be explained that the diluting gas has two important effects. The main effect was controlling the concentration of the copper vapors which led to a decrease the sizes of the powders. Another effect was the purging of the atmosphere inside the chamber. That is, the introduction of the diluting gas induced a decrease in of the oxygen concentration in the chamber and the pure copper powders were created by this effect.

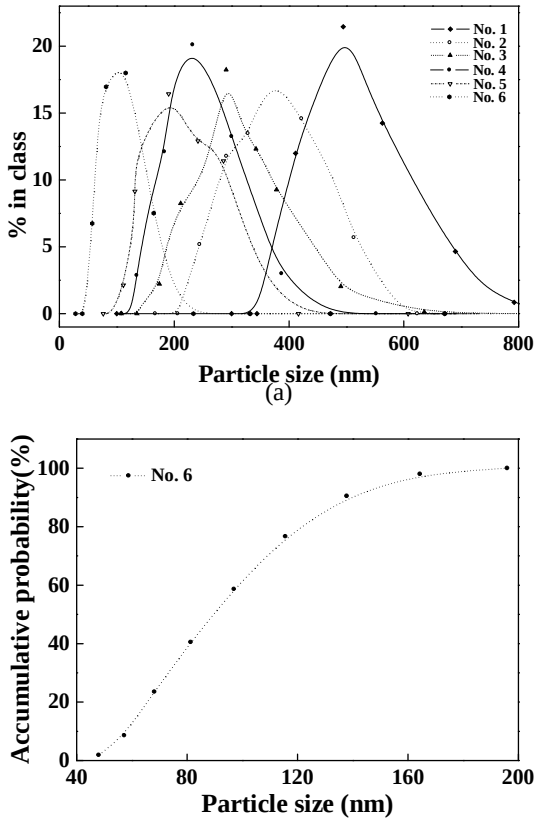

Fig. 4. (a) Particle size distributions of the powders synthesized at different diluting gas flow rates. (b) Accumulative probability of the powders at a diluting gas of 250 l/ min.

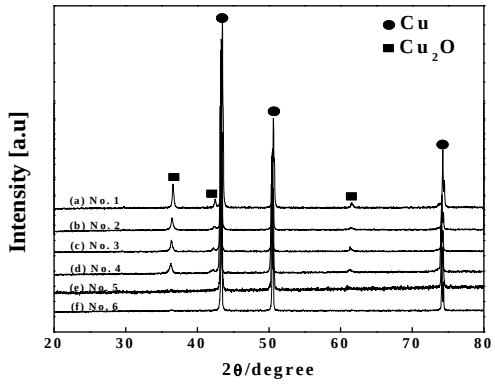

Fig. 5. X-ray diffraction patterns of powders prepared by transferred arc, depending on the diluting gas : (a) No. 1 (b) No. 2 (c) No. 3 (d) No. 4 (e) No. 5 (f) No. 6

The synthesized powders from experimental No. 5 and No. 6 were analyzed by Elemental Analyzer (EA) for an accurate phase composition analysis. An elemental analyzer can measure C, H, O, N, S weight percent within the purview of the whole sample weight. In this experiment, a little oxygen which was not verified from XRD data was detected 2.33 wt% and 1.18 wt% by EA, respectively. It could be reconfirmed that the synthesized powders from experimental No. 5 and No. 6 were almost all only copper nanopowders. Also, the contained oxygen was estimated as an oxide layer which was not copper oxide but an oxygen-coated copper nanopowder. Copper oxides stand for the chemical compounds of the copper such as CuO, Cu_2O. But oxygen-coated copper nanopowder means that it is pure metal surrounded by thin oxygen layer on the surface of the particles.

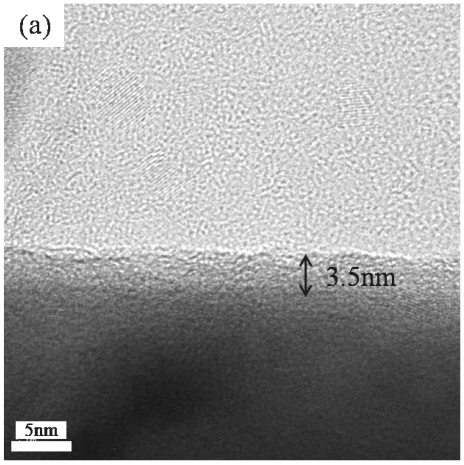

Fig. 6. TEM image of the powder depending on the diluting gas : (a) No. 6

Fig. 6 shows a high-resolution TEM image of the selected powder prepared at the same operating conditions as in experimental No. 6 to verify the existence of the oxygen-coated copper nanopowders. An external layer of about 3.5 nm thick was on the individual powder. It was estimated that the oxide layer and the prepared powder is the pure copper surrounded by the oxide layer. It was estimated that the oxide layer was created by the influx of the oxygen during the collecting process and the analyzing process, not during the quenching process.

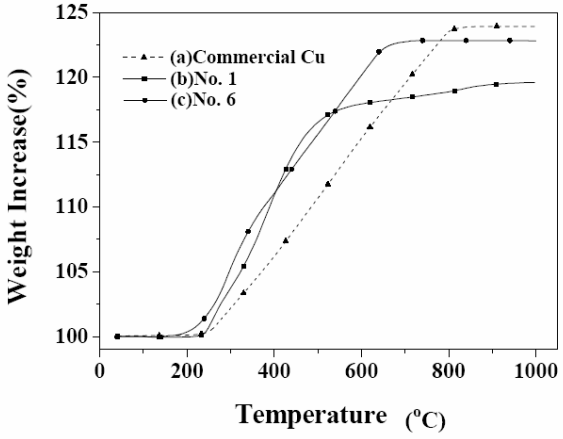

Fig. 7. TGA curves of commercial Cu and synthesized powders by transferred arc.

Fig. 7 presents TGA curves of the synthesized copper nanopowders for experimental No. 1 and No. 6. The copper powders were heated in oxygen at up to 1000 ℃ at a heating rate of 10℃/min, to inspect their resistances to oxidation at a high temperature. In the case of curve (c), oxidation started to increase in weight at approximately 180 ℃, and the weight increase leveled off 23 wt% at 700 ℃. Complete oxidation of the pure copper to the copper oxide (CuO) brings weight increase of about 24 wt%, and it showed curve (a). The weight increase shown by curves (a) and (c) were almost the same in TGA results, explained that the prepared powders were pure copper nanopowders. Also, the starting oxidation temperature depends on the powder sizes, and the surface areas. It means that the powder sizes were enough small and the particle surface area which come in contact with the oxygen is extensive, oxidation from pure metal to the metal oxide starts at a low temperature. Hence, the prepared powders were nano-sizes because of the low oxidation starting temperature.

3.2 SYSTEM 2 (Non-transferred arc plasma system)

Fig. 8 shows SEM images of the selected copper nanopowders prepared at the same operating conditions as in Table 2. When the N_2 added gas was introduced only 1 l/min to the chamber, the prepared powder sizes were below 200 nm. As the flow rate of the N_2 added gas was increased, the sizes of the prepared powders were increased. N_2 molecule is easily dissociated to atomic nitrogen and it partially generates the required heat for the evaporation of bulk copper through the recombination of the atomic nitrogen. For this reason, the concentration of the copper vapor inside chamber was increased and it caused increase the rate of the collision among the copper vapors. This phenomenon might lead to acceleration of nucleation. Thus, it was demonstrated that the effect of the N_2 added gas plays an important role to decide powder sizes. Also, the collection position is also an important factor in deciding powder sizes. The distance of the collection position from torch was represented in Fig. 2. According to the collection position, powder sizes were different in Fig. 8 (a), (d) and (e). Fig. 8 (a) showed that the sizes of the powder were smaller than those of Fig. 8 (d) and (e). As the collection position became more distant from torch, the sizes of the powders were increased.

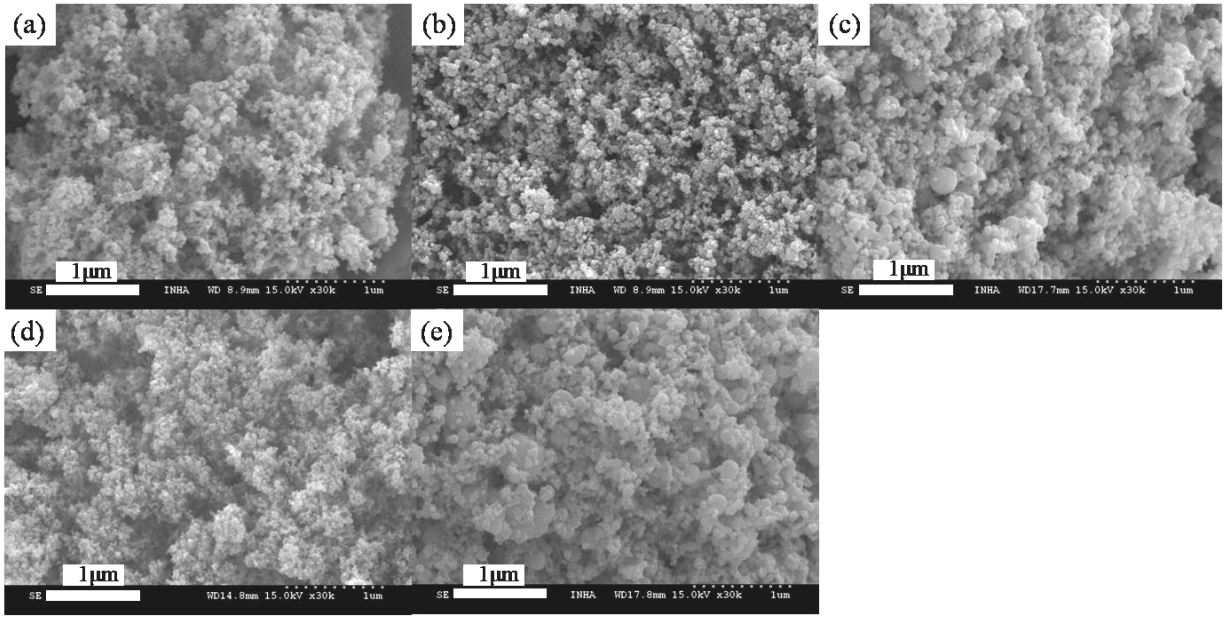

Fig. 8. SEM images of the powders obtained by non-transferred arc: (a) No. 7 (b) No. 8 (c) No. 9 (d) No. 10 (e) No. 11

Fig. 9 (a) shows the sizes of the powders according to the increase of N_2 as an added gas. As the flow rate of the N_2 added gas increased, the size of the prepared powder increased. Fig 9 (b) shows the sizes of the powder according to the collection position.

From No. 7 peaks, it can be demonstrated that the particle size was smaller and the particle distribution chart was narrower than those of No. 10 and No. 11 results.

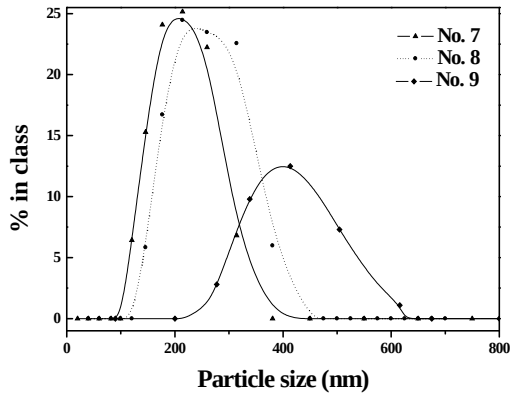

(a)

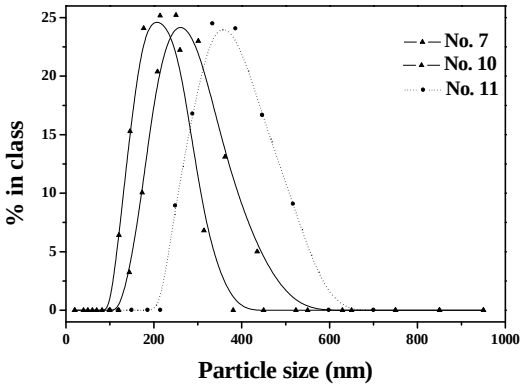

(b)

Fig. 9. (a) Particle size distributions of the powders synthesized at different N_2 added mass gas flow rates. (b) Particle size distributions of the powders synthesized in different collection positions.

Fig .10 shows the phase composition of the prepared powders by experimental No. 7, No. 10 and No. 11 depending on the collection position. When plasma torch was close to the collection position, the XRD peak of the prepared powders was a mixture of a large quantity of copper and a small amount of copper oxide (Cu_2O), corresponding to Fig .10 (c). However, as the distance became large, the oxidation level of the prepared powder has increased. Because the diluting gas was introduced nearby the bulk copper, the concentration of the oxygen at this position was lower than that of other locations. Thus, the oxidation level of the prepared powder obtained at this point was less than those of other powders. In this experiment, it was reconfirmed that the introduction of the diluting gas can control the oxidation level of the powders.

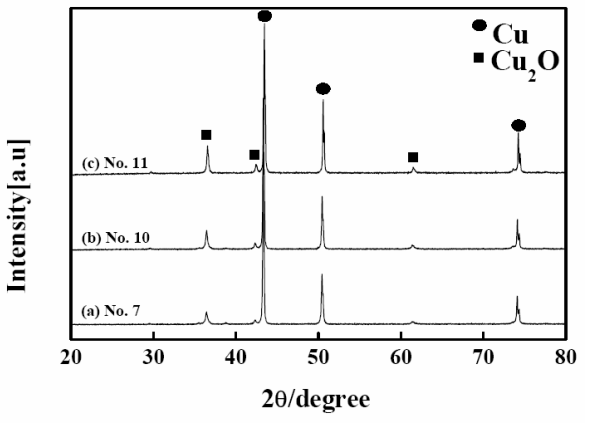

Fig. 10. X-ray diffraction patterns of the powders prepared by non-transferred arc depending on collection positions : (a) No. 7 (b) No. 10 (c) No. 11.

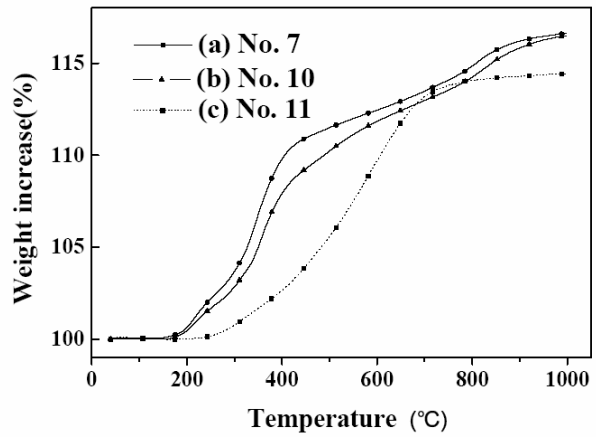

Fig. 11. TGA curves of the synthesized powders by non-transferred arc: (a) No. 7 (b) No. 10 (c) No. 11

Fig. 11 presents TGA curves of the synthesized powders by the non-transferred arc plasma system. In order to inspect their resistances to the oxidation at high temperatures the copper powders were heated in oxygen at up to 1000 ℃ at a heating rate of 10 ℃/min,. The same conditions were carried out in the system 1. The oxidation starting temperature of Fig. 11 (a) and (b) curves showed similar results, of around 180 ℃ approximately. The oxidation was terminated at approximately 950 ℃. It was argued before that the powder sizes collected according to No. 7 and No. 10 conditions were almost equal, and the corresponding curves are similar. However, the oxidation starting temperature shown by the curve from Fig. 11 (c) showed remarkably different results. As previously stated, the oxidation starting temperature depends on the particle sizes, and the surface areas. Hence, the No. 11 powder sizes were bigger and the oxidation level was much higher than for any other powders.

4. Conclusions

Copper nanopowders from bulk copper were successfully formed by a transferred arc plasma system and a non-transferred arc plasma system in this study. The diluting gas was introduced to restrain the nucleation and collision among copper vapors in case of the transferred arc plasma system. As the flow rate of the diluting gas was increased, the particle sizes of the prepared powder and the oxidation levels were decreased. Especially, when the flow rate of the diluting gas was introduced more than 200 l/min, most of the prepared powders were below 100 nm copper super-nanopowders as shown by XRD and EA results. Therefore, the introduction of the diluting gas is central factor in deciding on the special qualities such as the particle sizes and the oxidation levels in the transferred arc plasma system.

According to the flow rate of the N_2 added plasma gas, the particle sizes and the shapes of the prepared copper nanopowders were changed in the case of the non-transferred arc plasma system. The N_2 molecule is easily dissociated to atomic nitrogen and it partially generates the required heat for the evaporation of bulk copper through the recombination of the atomic nitrogen. It is known that this phenomenon is of a great help to increase the evaporation rate of metal [19]. As the flow rate of the N_2 added gas was increased, the formation rate and the particle sizes of the copper nanopowders were increased. Also, the oxidation levels of the powders were examined depending on the collection position in the non-transferred arc plasma system. Through the XRD and PSA results, it was demonstrated that the particle sizes and the characters of the copper nanopowders are highly depended on the collection position and the amount of a N_2 added gas.

In summary, through this study is shown that the thermal plasma systems may be suitable for the preparation and the mass production of copper nanopowders. However, the non-transferred arc plasma system needs bimolecular compounds such as H_2 and N_2 for the rapid evaporation, and the evaporation rate was also below that of the transferred arc plasma system. Therefore, a transferred arc plasma system used in making metal nanopowders from bulk material is better than that of the non-transferred arc system. This work confirms the possibility of commercially production of metal powder through improvements of thermal plasma systems.

Acknowledgements

This study was supported by the Regional Innovation Center for Environmental Technology of Thermal Plasma (ETTP) at Inha University designated by MKE(2009).

References

[1] Testu Yonezawa, Masanori Tomonari, Nanotechnology **19**, 145706 (2008).
[2] Xinjun Wang, Kai Jiang, Mater.Let. **62**, 3509 (2008).
[3] P. Matteazzi, D. Basset, E. Miani, G. Le Cair, Nanostru. Mat. **2**, 217 (1993).
[4] W. J. Hwa, S. D. Lee, Y. B. Lee, H. C. Park, K. H. Kim, S. S. Park, J. Koran Ind. Eng. Chem. **15**(7), 715 (2004).
[5] C. D. Terwiiliger, Y.-M. Chiang, Nanostru.Mater. **4**(6), 651 (1994).
[6] S. Stopic, J. Nedeljkovi´c, Z. Rako˘cevic, D. Uskokovic, J. Mater. Res. **14**(7), 3059 (1999).
[7] J. E. Lee, S. M. Oh, D. W. Park, Thin Solid Films, **457**, 230 (2004).
[8] M. Vijay, V. Selvarajan, Journal of Mater. Pro.Tech, **202**,112 (2008).
[9] L. Tong, R. G.Reddy Scripta Mat. **52**, 1253 (2005).
[10] Y. Moriysohi, M. Futaki, S. Komatsu, T. Ishigaki., J. Mater Sci Lett., **16**, 347 (1997).
[11] O. Fukumasa, T. Fujiwara, Thin Solid Films, **435**, 33 (2003).
[12] C. Chazelas, J. F. Coudert, J. Jarrige, P. Fauchais, J Eur Ceram Soc, **27**, 947 (2007).
[13] M. T. Swihart Curr Opin Colloid Interface Sci., **8**, 127 (2003).
[14] S. H. Lee, S. M. Oh, D. W. Park, Mater Sci Eng C. **27**,1286 (2007).
[15] Taegong Ryu, Zhigang Z. Fang, Int. Journal of Refractory Metals & Hard Materials, **27**,149 (2009).
[16] I. Mohai, J Szepvogyi, Chemical Engineering and Processing, **44,** 225 (2005).
[17] N. Kobayashi, T. Ishigaki, Thin Solid Films, **516**, 4402 (2008).
[18] Um, M. H., Lee, C. T. H. Kumazawa, J. Mater. Sci. Let. **16**, 344 (1997).
[19] S. M. Oh, D. W.Park, J. Koran Ind. Eng.Chem. **16**(3), 132 (2003).

*Corresponding author: dwpark@inha.ac.kr